# ONE-DIMENSIONAL MAPPINGS FOR RECOVERING LARGE SCALE PROJECTIVE TRANSFORMATIONS

*Zhang Yun, Henry Chu*

Center for Advanced Computer Studies, The University of Louisiana at Lafayette, U.S.A.

## ABSTRACT

One-dimensional mappings in the log-polar and in the inverse-polar spaces are proposed. Based on these mappings, a two-step search strategy has been developed to recover the eight parameters of a general projective transformation between two image patches. First, the four affine parameters are recovered using the one-dimensional log-polar mapping. Secondly, the two projective parameters are recovered using the one-dimensional inverse-polar mapping. At each step the recovery is done by mapping only two line pairs. The remaining two translational parameters are determined by applying these two mappings to an exhaustive search. The proposed mapping strategy has successfully been used to recover different two-dimensional transformations between real images.

***Index Terms*—** image registration, video coding, image motion analysis, stereo vision, correspondence problem.

## 1. INTRODUCTION

Image registration and matching features from different images is a fundamental image processing task with applications in video processing and computer vision. The goal of image mapping is to find a geometric transformation between two image patches of the same scene taken from different locations (or view points) and/or at different times. Because it is often the first step to a variety of tasks in image processing and computer vision, a flexible and robust approach to image mapping becomes crucial.

Much research has been done on image registration for over twenty years [1]. A general framework of image mapping proposed in [2] consists of four components: feature space, similarity measure, search space and search strategy. Based on which feature space and search strategy are employed, there are two different approaches that have been developed to match images under large deformations. They can be referred to as the intensity-based optimal search [8, 6, 1, 5, 12] and feature-based exhaustive search [13, p. 195 and p. 155, 7, 9, 10]. Some promising results have been obtained when the deformation is small. For example, the transformation could be recovered using nonlinear methods in the case where the shift between two image patches is within a few (e.g., 2 or 3) pixels [5]. On the other hand, when the transformation is of a larger scale, it is possible that a nonlinear method will reach a local rather than a global solution. Thus, in order for a nonlinear method to succeed a good initial solution from a linear search is necessary. The state-of-the-art in a linear search can only be applied to the cases of finding translations [11, p. 155] or similarity transformations [12].

To describe a large scale deformation, we need a projective or at least an affine transformation model [3, p. 251, 11, p. 133]. In this work we focus on developing a flexible and efficient linear search strategy to recover a large affine/projective transformation. The contributions of the present work are that two novel one-dimensional (1-D) mappings are proposed. We use these mappings in a two-step search strategy to recover the eight parameters of a general projective transformation. In the first step, the four affine parameters (i.e., the upper left part of the projective projection matrix) are recovered using the 1-D log-polar mapping. In the second step, the two projective parameters (i.e., the bottom row of the projective projection matrix) are recovered using the 1-D inverse-polar mapping. It is noted that at each step the recovery is done by mapping only two pairs of line segments. Finally, the remaining two translational parameters can be determined by combined the 1-D mappings with an exhaustive search method.

## 2. 1D MAPPINGS

Suppose there exists a 2-D projective transformation between a source image patch and a target image patch. If the origins of the local image frames are set at the centers of these patches, the transformation between a source point, $\mathbf{x}\left(=[x, y]^T\right)$, and its target counterpart, $\mathbf{x}'\left(=[x', y']^T\right)$, can be expressed as:

$$\begin{bmatrix} x' \\ y' \\ 1 \end{bmatrix} = \begin{bmatrix} a & b & 0 \\ c & d & 0 \\ e & f & 1 \end{bmatrix} \begin{bmatrix} x \\ y \\ 1 \end{bmatrix}, \tag{1}$$

which is a general eight-parameter projective transformation represented by the four affine parameters $a$, $b$, $c$ and $d$, the two projective parameters $e$ and $f$; note that the two translational parameters are set to zero when we center the image patches. Consider a collection of line segments that pass through the center of the patch. Then each point is located along a 1-D radial line rather than in a 2-D area. In particular, if $\mathbf{x}$ is on a source radial line represented by $y = kx$, where $k$ is the slope of the line, Eq. (1) can be rewritten as:

$$x' = \frac{(a+bk)x}{(e+fk)x+1}; \qquad y' = \frac{(c+dk)x}{(e+fk)x+1}. \tag{2}$$

If the set of radial lines has sufficient coverage of the image patch, the transformation of the entire patch can be inferred from the transformation of radial lines.

### 2.1. Recovery of four affine parameters

There are six parameters given in Eq. (1) that need to be recovered. In this section, we propose a 1-D mapping in the log-polar space that can be used to recover the four affine parameters, $a$, $b$, $c$ and $d$. By manipulating Eq. (2), we have a set of two equations about the affine parameters:

$$\begin{aligned} k' &= \frac{c+dk}{a+bk} \\ \log_t r' &= \frac{1}{2}\log_t \frac{(a+bk)^2+(c+dk)^2}{1+k^2}, \\ &\quad -\log_t |(e+fk)x+1| + \log_t r \end{aligned} \tag{3}$$

where $k'$ is the slope of the transformed radial line, $r\left(=\sqrt{(1+k^2)}|x|\right)$ is the radial distance of $\mathbf{x}$, $r'\left(=\sqrt{x'^2+y'^2}\right)$ is the radial distance of $\mathbf{x}'$, and $t$ is the logarithmic base.

In recovering the four affine parameters, the term that contains the two projective parameters, $\log_t |(e+fk)x+1|$, becomes a measurement error, which is negligible if a small image patch is used. This observation has been verified with the experimental results.

From Eq. (3), we see that the slope and radial shift of the transformed line can be determined by mapping a pair of two radial lines in the log-polar space. The search space for such a mapping is two-dimensional since we need to search for two parameters, i.e., radial angle and radial shift. Further, one mapping gives two constraints for the four unknown affine parameters. Thus, in order to recover these parameters we need to perform at least two mappings of this kind and then solve for $a$, $b$, $c$ and $d$.

A system of equations formed by the slopes $k_i'$, and radial shifts, $s_i$, of two line pairs is given by:

$$\begin{aligned} &c+dk_i = k_i'(a+bk_i); \\ &(a+bk_i)^2+(c+dk_i)^2 = (1+k_i^2)^{2s_i} \end{aligned} \tag{4}$$

with $i = 1, 2$. By solving the above system of equations, we can determine the four affine parameters, $a$, $b$, $c$ and $d$, as follows:

$$\begin{aligned} a &= \frac{1}{k_2-k_1}(k_2u_1-k_1u_2); \qquad b = \frac{1}{k_2-k_1}(u_2-u_1) \\ c &= \frac{1}{k_2-k_1}(k_2v_1-k_1v_2); \qquad d = \frac{1}{k_2-k_1}(v_2-v_1) \end{aligned} \tag{5}$$

where $u_i$ and $v_i$ with $i = 1, \cdots, 4$ are intermediate parameters determined as:

$$u_i = \pm\sqrt{\frac{(1+k_i^2)^{2s_i}}{1+k_i'^2}}; \qquad v_i = \pm k_i'\sqrt{\frac{(1+k_i^2)^{2s_i}}{1+k_i'^2}}. \tag{6}$$

The signs of $u_i$ and $v_i$ can be determined based on the detected radial angles for the matching target lines.

### 2.2. Recovery of two projective parameters

Once the four affine parameters have been determined, the next task is to recover the two projective parameters, $e$ and $f$. A 1-D mapping in the inverse-polar space can be used to accomplish this task. By a different manipulation of the two equations given in Eq. (2), we have a set of two equations about the projective parameters as follows:

$$k' = \frac{c+dk}{a+bk} \tag{7a}$$

$$\frac{1}{r'} = \operatorname{sgn}(\cos\theta)\frac{e+fk}{\sqrt{(a+bk)^2+(c+dk)^2}} + \frac{\sqrt{1+k^2}}{\sqrt{(a+bk)^2+(c+dk)^2}}\frac{1}{r} \tag{7b}$$

where sgn denotes the signum function and $\theta$ is the radial angle at which the source line lies.

Under a two-parameter projective transformation a radial line does not change its radial angle (Eq. (7a)). However, it does shift in the radial direction and this radial shift is antisymmetric about the origin (Eq. (7b)).

In order to recover these two parameters we need to perform at least two mappings of this kind and then solve for $e$ and $f$ a system of the equations formed by using the detected radial shifts of transformed lines. After two radial shifts, $s_i$, have been detected from one-dimensional searches, we can solve the following two equations,

$$e + fk_i = \operatorname{sgn}(\cos\theta_i)s_i\sqrt{(a+bk_i)^2+(c+dk_i)^2}, \; i = 1,2, \tag{8}$$

for the two projective parameters, $e$ and $f$:

$$\begin{aligned} e = \frac{1}{k_2-k_1}\Big\{ &k_2 \operatorname{sgn}(\cos\theta_1)\sqrt{(a+bk_1)^2+(c+dk_1)^2}\,s_1 \\ &-k_1 \operatorname{sgn}(\cos\theta_2)\sqrt{(a+bk_2)^2+(c+dk_2)^2}\,s_2 \Big\} \end{aligned} \tag{9a}$$

$$\begin{aligned} f = \frac{1}{k_1-k_2}\Big\{ &\operatorname{sgn}(\cos\theta_1)\sqrt{(a+bk_1)^2+(c+dk_1)^2}\,s_1 \\ &-\operatorname{sgn}(\cos\theta_2)\sqrt{(a+bk_2)^2+(c+dk_2)^2}\,s_2 \Big\}. \end{aligned} \tag{9b}$$

### 2.3. The Algorithm

To briefly summarize, the algorithm for recovering the parameters of a projective transformation is as follows. The registration between two image patches consists of an iteration of the following steps in the search range for the center of a matching target image patch using the exhaustive search method:

1. 1-D log-polar mapping: determine the center of the matching target image patch and the 4 affine parameters, which has the following steps:
   a. Transform source line segments and the target image patch to the log-polar space (Eq. (3)).
   b. Match each source line segment to its target counterpart in the log-polar space to obtain angle and radial shift of the target line segment (Eq. (3)).
   c. Compute the four affine parameters using the obtained angles and radial shifts (eqs. (5) and (6)).
2. 1-D inverse-polar mapping: determine the 2 projective parameters, which has the following steps:
   a. Transform source line segments and the target counterparts to the inverse-polar space (Eq. (7)).
   b. Match these pairs of line segments in the inverse-polar space to obtain radial shifts of the target line segments (Eq. (7)).
   c. Compute the 2 projective parameters using the obtained radial shifts (Eq. (9)).
3. Compute similarity of the two image patches. If the similarity is higher, update the record of the results, viz. the center of the matching target patch and the other 6 parameters of the projective transformation.

It is worth noting that in the implementation of the above algorithm, we match four source radial lines as evaluated by the NCC similarity measure. From these four matches we can obtain altogether six sets of solutions for $a$, $b$, $c$, $d$, $e$ and $f$. The final solution for these parameters is an average of the solutions.

## 3. EXPERIMENTAL RESULTS

The performance of the 1-D mappings is evaluated using a similarity measure (NCC) computed for each of two matching image patches. The images “bark” and “graf” given in [13] are used for testing. The image patches are circular with radius 56. The source image patches are cropped at the center of the image. Thus, the center is at (382, 256) for “bark” and at (400, 320) for “graf.” For each source image patch, four radial line segments at 0°, 45°, 90° and 135° are chosen to be matched to their counterparts in target images. The dimension of the transformed images in the log-polar space is set to 224×360, while in the inverse-polar space is set to 9821×360. The warping between images is performed using the bilinear interpolation. The center of the target image patch is determined by exhaustively searching through a small range of [-6, 6] around a pre-estimated value.

In the following two subsections, we present the results of the recovery of the transformations for the zoom and rotation, and for the viewpoint changes.

### 5.1 Recovery of transformations for zoom and rotation

Two real image pairs have been tested. The recovered transformations are given in Table 1 as Transformations (9) and (10). The source image patch is shown in Figure 1(a).The image registration results are shown in Figures 1(b) and (c). The similarity measures in these two cases are 0.945064 and 0.812915. Since a large optic zoom (about 4×) exists in the image pair shown in Figures 1(a) and (c), the similarity obtained in this case can still be considered as good.

**Table 1 Recovered transformations for real image pairs.**

| No. | Transformation Matrix | Center |
|---|---|---|
| 9 | -0.204854 0.343770 0.000000<br>-0.354817 -0.202495 0.000000<br>0.000041 0.000080 1.000000 | 260 284 |
| 10 | -0.219190 -0.148420 0.000000<br>0.140366 -0.212022 0.000000<br>0.000411 -0.001164 1.000000 | 471 348 |
| 11 | 0.427458 0.598612 0.000000<br>-0.255641 0.839033 0.000000<br>0.000279 0.000350 1.000000 | 388 345 |
| 12 | 0.215819 -0.545056 0.000000<br>0.199573 0.895796 0.000000<br>0.000088 0.000026 1.000000 | 346 384 |

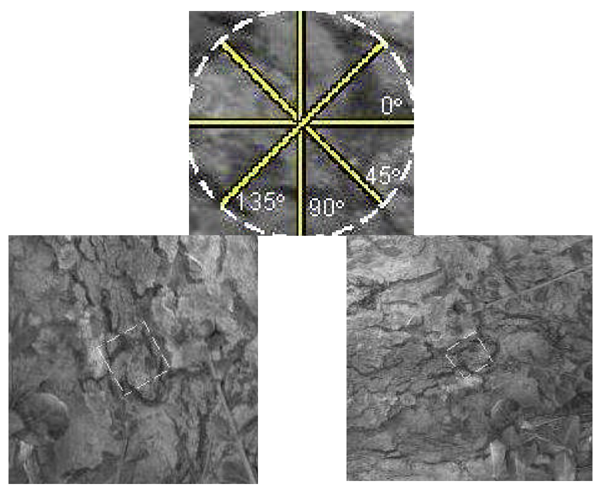


**Figure 1 (a) Source image patch "bark" and four radial lines (*top*), and registration results highlighted on real target images (b) (*lower left*) and (c) (*lower right*).**

### 5.2 Recovery of transformations for viewpoint changes

Two real image pairs have been tested. The recovered transformation matrices are given in Table 1 as Transformations (11) and (12). The source image patch is given in Figure 2(a). To visualize the effect of the recovery, the image registration results are shown in Figures 2(b) and (c). The similarity measures in these two cases are 0.978086 and 0.942173, both of which are high.

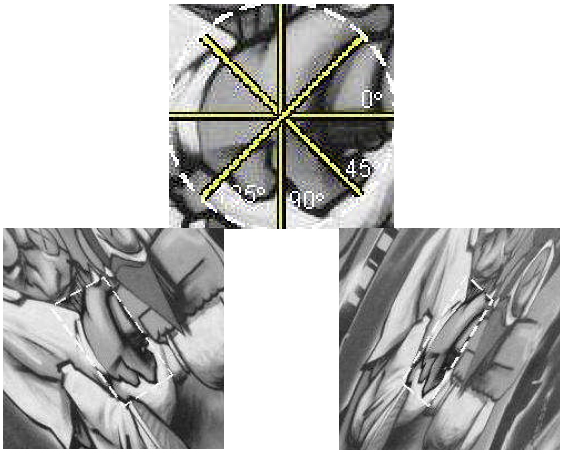


**Figure 2 (a) Source image patch "graf" and four radial lines (*top*), and registration results highlighted on real target images (b) (*lower left*) and (c) (*lower right*).**

## 4. CONCLUDING REMARKS

We presented analyses and experimental results to show that the 1-D mappings can be used to recover large similarity/affine/projective transformations. We note that while the previously proposed block log-polar mapping [12] can be used to recover similarity transformations, it cannot be used by itself to recover the affine/projective transformations. Compared to the 2-D mapping, the proposed 1-D mappings are more flexible in that it can be applied to recover a general projective projection matrix. Furthermore, it is computationally efficient because the recovery can be done by mapping only two line pairs.

Secondly, the image "graf" has been demonstrated to be problematic for the block mapping using a nonlinear search method [6]. Using the proposed 1-D mapping, we observed that it is easy to find a matching and the obtained similarity measure is very high. Heavily textured images like "graf" may have many local minima that prevent the nonlinear search from reaching the global one. In contrast, this kind of fine texture is a useful aid to the 1-D mappings.

As the immediate future work, it is possible to extend the present work to a multiscale-based approach to recover the translation in a large search area.

## REFERENCES

[1] S. Baker, and I. Matthews, "Lucas-Kanade 20 Years On: A Unifying Framework," *Int. J. Comput. Vis.*, vol. 56, pp. 221-255, 2004.

[2] L. G. Brown, "A Survey of Image Registration Techniques," *ACM Computing Surveys*, vol. 24, no. 4, pp. 325-376, Dec. 1992.

[3] O. Faugeras, Q.-T. Luong, and T. Papadopoulo, *The Geometry of Multiple Images*, The MIT Press, 2001.

[4] M. A. Fischler, and R. C. Bolles, "Random Sample Consensus: A Paradigm for Model Fitting with Applications to Image Analysis and Automated Cartography," *Comm. Assoc. Comp. Mach.*, vol. 24, no. 6, pp 381-395, 1981.

[5] B. Georgescu, and P. Meer, "Point Matching under Large Image Deformations and Illumination Changes," *IEEE Trans. Pattern Recognition Analysis Machine Intelligence*, vol. 26, pp. 674-688, 2004.

[6] B. Horn, and B. Schunck, "Determining Optical Flow," *Artificial Intelligence*, vol. 17, pp. 185-203, 1981.

[7] D. Lowe, "Distinctive Image Features from Scale-Invariant Keypoints," *Int. J. Comput. Vis.*, vol. 60, pp. 91-110, 2004.

[8] B. Lucas, and T. Kanade, "An Iterative Image Registration Technique with An Application to Stereo Vision," *Proc. 7th International Joint Conference on Artificial Intelligence*, Vancouver, Canada, pp674-679, 1981.

[9] K. Mikolajczyk, T. Tuytelaars, C. Schmid, A. Zisserman, J. Matas, F. Schaffalitzky, T. Kadir, and L. Van Gool, "A Comparison of Affine Region Detectors," *Int. J. Comput. Vis.*, vol. 65, pp. 43-72, 2005.

[10] P. H. S. Torr, and A. Zisserman, "Robust Computation and Parameterization of Multiple View Relation," *Proc. 6th Int. Conference on Computer Vision*, Bombay, India, pp. 727-732, 1998.

[11] Y. Wang, J. Ostermann, and Y.-Q. Zhang, *Video Processing and Communications*, Prentice Hall, 2002.

[12] S. Zokai, and G. Wolberg, "Image Registration Using Log-Polar Mappings for Recovery of Large-Scale Similarity and Projective Transformation," *IEEE Trans. Image Processing*, vol. 14, pp. 1422-1434, 2005.